Prepared for submission to JHEP KIAS-P12056

Can Zee-Babu model implemented with scalar dark matter explain both Fermi/LAT 130 GeV γ-ray excess and neutrino physics ?

Seungwon Baek[a] **P. Ko,**[a] **and Eibun Senaha**[a]

[a] *School of Physics, KIAS, Seoul 130-722, Korea*

E-mail: swbaek@kias.re.kr, pko@kias.re.kr, senaha@kias.re.kr

Abstract: We implement the Zee-Babu model for the neutrino masses and mixings by incorporating a scalar dark matter X. The singly and doubly charged scalars that are new in the Zee-Babu model can explain the large annihilation cross section of a dark matter pair into two photons as hinted by the recent analysis of the Fermi γ-ray space telescope data, if new charged scalars are relatively light and have large couplings to a pair of dark matter particles. These new scalars can also enhance the $B(H \to \gamma\gamma)$, as the recent LHC results may suggest. The dark matter relic density can be explained. The direct detection rate of the dark matter is predicted to be about one order of magnitude down from the current experimental bound. However, it turns out that neutrino masses are too small within the parameter space fitting the 130 GeV γ-ray excess. There should be additional contributions to the neutrino masses and mixings without new extra charged particles, and the Type-I seesaw can do this job.

Keywords:

Contents

1 Introduction

Although it is well known that the dark matter (DM) constitutes about 23% of the total mass density of the universe, *i.e.* $\Omega_{\rm DM}h^2 = 0.1123 \pm 0.0035$ [1], its existence has only been inferred from the gravitational interaction. And its nature is still unknown. If the DM is weakly interacting massive particle (WIMP), it may reveal itself via non-gravitational interactions, for example, by pair annihilation into ordinary standard model (SM) particles including photon [2]. In this case, the relic DM abundance is roughly related to the pair annihilation cross section at freezeout, $\langle\sigma v\rangle_{\rm th}$, as

$$\Omega_{\rm DM}h^2 = \frac{3\times 10^{-27}{\rm cm}^3/{\rm s}}{\langle\sigma v\rangle_{\rm th}}. \tag{1.1}$$

Recently Refs. [3, 4] claim that the Fermi γ-ray space telescope may have seen excess of the photons with $E_\gamma \sim 130$ GeV from the center of the Milky Way compared with the background. Interpreting its origin as the annihilation of a pair of DM particles, they could obtain the annihilation cross section to be about 4% of that at freezeout:

$$\langle\sigma v\rangle_{\gamma\gamma} = 0.042\langle\sigma v\rangle_{\rm th} = 0.042\ {\rm pb}\, c. \tag{1.2}$$

Since DM is electrically neutral, the pair annihilation process into photons occurs through loop-induced diagrams. Naively we expect

$$\frac{\langle\sigma v\rangle_{\gamma\gamma}}{\langle\sigma v\rangle_{\rm th}} = \left(\frac{\alpha_{\rm em}}{\pi}\right)^2 \sim 10^{-5}. \tag{1.3}$$

So the observed value in (1.2) is rather large, and we may need new electrically charged particles running inside the loop beyond the SM. Many new physics scenarios were speculated within various CDM models by this observation [5].

The so-called 'Zee-Babu model' [7–9] provides new charged scalars, h^+, k^{++} at electroweak scale, in addition to the SM particles. These new charged scalars carry two units of lepton number and can generate Majorana neutrino masses via two-loop diagrams. The diagrams are finite and calculable. The neutrino masses are naturally small without the need to introduce the right-handed neutrinos for seesaw mechanism. One of the neutrinos is predicted to be massless in this model. Both normal and inverse hierarchical pattern of neutrino masses are allowed. The observed mixing pattern can also be accommodated. The model parameters are strongly constrained by the neutrino mass and mixing data, the radiative muon decay, $\mu \to e\gamma$, and $\tau \to 3\mu$ decay [10].

It would be very interesting to see if the new charged particles in the Zee-Babu model can participate in some other processes in a sector independent of neutrinos. In this paper, we minimally extend the Zee-Babu model to incorporate the DM (See also [11]). We introduce a scalar dark matter X with a discrete Z_2 symmetry under which the dark matter transforms as $X \to -X$ in order to guarantee its stability. The renormalizable interactions between the scalar DM X with the Higgs field and the Zee-Babu scalar fields provide a Higgs portal between the SM sector and the DM. We show that the Zee-Babu scalars and their interactions with the DM particle can explain the gamma-ray excess as well as the DM relic density. The branching ratio of Higgs to two photons, $B(H \to \gamma\gamma)$, can also be enhanced as implied by the recent LHC results [12]. The spin-independent cross section of the dark matter scattering off the proton, σ_p, is less than about 1×10^{-9} pb, which can be probed at next generation searches.

This paper is organized as follows. In Section 2, we define our model by including the scalar DM in the Zee-Babu model, and consider theoretical constraints on the scalar potential. In Section 3, we study various DM phenomenology. We calculate the dark matter relic density and the annihilation cross section $\langle\sigma v\rangle_{\gamma\gamma}$ in our model. We also predict the cross section for the DM and proton scattering. We also predict the branching ratio for the Higgs decay into two photons, $B(H \to \gamma\gamma)$. And we consider the implication on the neutrino sector. We conclude in Section 4.

2 The model and theoretical constraints on the scalar potential

2.1 Implementation of Zee-Babu model with scalar dark matter

We implement the Zee-Babu model for radiative generation of neutrino masses and mixings, by including the scalar DM X with Z_2 symmetry $X \to -X$. All the possible renormalizable interactions involving the scalar fields are given by

$$\mathcal{L} = \mathcal{L}_{\text{Babu}} + \mathcal{L}_{\text{Higgs+DM}} \tag{2.1}$$

$$\mathcal{L}_{\text{Babu}} = f_{ab} l_{aL}^{Ti} C l_{bL}^{j} \epsilon_{ij} h^+ + h'_{ab} l_{aR}^{T} C l_{bR} k^{++} + H.c. \tag{2.2}$$

$$-\mathcal{L}_{\text{Higgs+DM}} = \lambda_H (H^\dagger H)^2 + \frac{1}{4}\lambda_X X^4 + \lambda_h (h^+ h^-)^2 + \lambda_k (k^{++} k^{--})^2$$

$$
\begin{aligned}
&+ \frac{1}{2}\lambda_{HX} H^\dagger H X^2 + \lambda_{Hh} H^\dagger H h^+ h^- + \lambda_{Hk} H^\dagger H k^{++} k^{--} \\
&+ \frac{1}{2}\lambda_{Xh} X^2 h^+ h^- + \frac{1}{2}\lambda_{Xk} X^2 k^{++} k^{--} + \lambda_{hk} h^+ h^- k^{++} k^{--} \\
&+ (\mu_{hk} h^+ h^+ k^{--} + h.c) \\
&- \mu_H^2 H^\dagger H + \frac{1}{2}\mu_X^2 X^2 + \mu_h^2 h^+ h^- + \mu_k^2 k^{++} k^{--}.
\end{aligned} \tag{2.3}
$$

Note that our model is similar to the recent model proposed by J. Cline [6]. However we included the interaction between the new charged scalar and the SM leptons that are allowed by gauge symmetry, and thus the new charged scalar bosons are not stable and cause no problem.

The original Zee-Babu model was focused on the neutrino physics, and the operators of Higgs portal types were not discussed properly. It is clear that those Higgs portal operators we include in the 2nd line of (2.3) can enhance $H \to \gamma\gamma$, without touching any other decay rates of the SM Higgs boson, as long as $h^\pm$ and $k^{\pm\pm}$ are heavy enough that the SM Higgs decays into these new scalar bosons are kinematically forbidden.

2.2 Constraints on the potential

We require μ_X^2, μ_h^2 and μ_k^2 to be positive. Otherwise the imposed Z_2 symmetry $X \to -X$ or the electromagnetic U(1) symmetry could be spontaneously broken down. Since the masses of X, k^{++} and h^+ have contributions from the electroweak symmetry breaking as

$$
\begin{aligned}
m_X^2 &= \mu_X^2 + \frac{1}{2}\lambda_{HX} v^2, \\
m_{h^+}^2 &= \mu_h^2 + \frac{1}{2}\lambda_{Hh} v^2, \\
m_{k^{++}}^2 &= \mu_k^2 + \frac{1}{2}\lambda_{Hk} v^2,
\end{aligned} \tag{2.4}
$$

we obtain the conditions on the quartic couplings

$$
\lambda_{HX} < \frac{2m_X^2}{v^2}, \quad \lambda_{Hh} < \frac{2m_{h^+}^2}{v^2}, \quad \lambda_{Hk} < \frac{2m_{k^{++}}^2}{v^2}. \tag{2.5}
$$

We note that the above conditions are automatically satisfied if the couplings takes negative values. In such a case, however, we also need to worry about the behavior of the Higgs potential for large field values. For example, if we consider only the neutral Higgs field, H[1], and the dark matter field, X, we get

$$
\begin{aligned}
V &\sim \frac{1}{4}\lambda_H H^4 + \frac{1}{4}\lambda_X X^4 + \frac{1}{4}\lambda_{HX} H^2 X^2, \\
&\sim \frac{1}{4}\begin{pmatrix} H^2 & X^2 \end{pmatrix} \begin{pmatrix} \lambda_H & \frac{1}{2}\lambda_{HX} \\ \frac{1}{2}\lambda_{HX} & \lambda_X \end{pmatrix} \begin{pmatrix} H^2 \\ X^2 \end{pmatrix},
\end{aligned} \tag{2.6}
$$

for large field values of H and X. If the potential is to be bounded from below, every eigenvalue of the square matrix of the couplings in (2.6) should be positive, whose condition

[1] We use the same notation with the Higgs doublet.

is

$$|\lambda_{HX}| < \sqrt{4\lambda_H \lambda_X}. \tag{2.7}$$

This means that even if λ_{HX} is negative, its absolute value should not be arbitrarily large because $\lambda_H = m_H^2/2v^2 \approx 0.13$ ($m_H \approx 125$ GeV) and λ_X is bounded from above so as not to generate the Landau pole. For example, the renormalization group running equations (RGEs) of λ_H, λ_X and λ_{HX} are given by

$$\begin{aligned}
\frac{d\lambda_H}{d\log Q} &= \frac{1}{16\pi^2}\left(24\lambda_H^2 + \frac{1}{2}\lambda_{HX}^2\right) + \cdots, \\
\frac{d\lambda_X}{d\log Q} &= \frac{1}{16\pi^2}\left(18\lambda_X^2 + 2\lambda_{HX}^2\right) + \cdots, \\
\frac{d\lambda_{HX}}{d\log Q} &= \frac{\lambda_{HX}}{8\pi^2}\left(6\lambda_H + 3\lambda_X\right) + \cdots,
\end{aligned} \tag{2.8}$$

where the dots represents other contributions which are not important in the discussion. The complete forms of the β-functions of the quartic couplings are listed in Appendix A.

The approximate solution for λ_X in (2.8) shows that the Landau pole is generated at the scale $Q = Q_{\rm EW}\exp\left(1/\beta_H \lambda_X(Q_{\rm EW})\right)$ ($\beta_H = 18/16\pi^2$). If we take the electroweak scale value of the Higgs quartic coupling to be $\lambda_X(Q_{\rm EW}) \sim 5$, the cut-off scale should be around 1 TeV. The general condition for the bounded-from-below potential for large field values is that all the eigenvalues of the matrix

$$\begin{pmatrix}
\lambda_H & \frac{1}{2}\lambda_{HX} & \lambda_{Hh} & \lambda_{Hk} \\
\frac{1}{2}\lambda_{HX} & \lambda_X & \lambda_{Xh} & \lambda_{Xk} \\
\lambda_{Hh} & \lambda_{Xh} & 4\lambda_h & 2\lambda_{hk} \\
\lambda_{Hk} & \lambda_{Xh} & 2\lambda_{hk} & 4\lambda_k
\end{pmatrix} \tag{2.9}$$

should be positive.

In the following discussion, we require that all scalar quartic couplings (λ_i) be perturbative up to some scale Q. To this end, we solve the one-loop RGEs of those quartic couplings given in Appendix A. For the moment, we do not include new Yukawa couplings defined in Eq. (2.2), and we adopt the criterion $\lambda_i(Q) < 4\pi$ in this analysis. In Fig. 1, the perturbativity bounds are shown in the $\lambda_{Xh(k)}$-$\lambda_{Hh(k)}$ plane. We take $Q = 1$, 3, 10 and 15 TeV, which are denoted by the red curves from top to bottom. For other parameters, we fix $\lambda_{Hh} = \lambda_{Hk}$, $\lambda_{Xh} = \lambda_{Xk}$, $\lambda_{hk} = \lambda_{HX} = 0$ and $\lambda_X = \lambda_H (\simeq 0.13)$. As explained above, a certain negative value of $\lambda_{Hk(h)}$ may cause the instability of the Higgs potential. To avoid this, we set $\lambda_h = \lambda_{Hh}^2/(2\lambda_H)$ and $\lambda_k = \lambda_{Hk}^2/(2\lambda_H)$ for $\lambda_{Hk(h)} < 0$. For $\lambda_{Hk(h)} > 0$, on the other hand, $\lambda_h = \lambda_k = \lambda_H$ is taken. As we see from the plot, $\lambda_{Xk(h)} \simeq 7 - 11$ is possible if $Q = 1$ TeV.

The theoretical arguments (2.5) and (2.7) restrict λ_{HX} to lie roughly to the range, $(-1.6, 0.6)$. Similarly, we have $\lambda_{Hh(k)} \lesssim 0.7$ for $m_{h^+(k^{++})} = 150$ GeV.

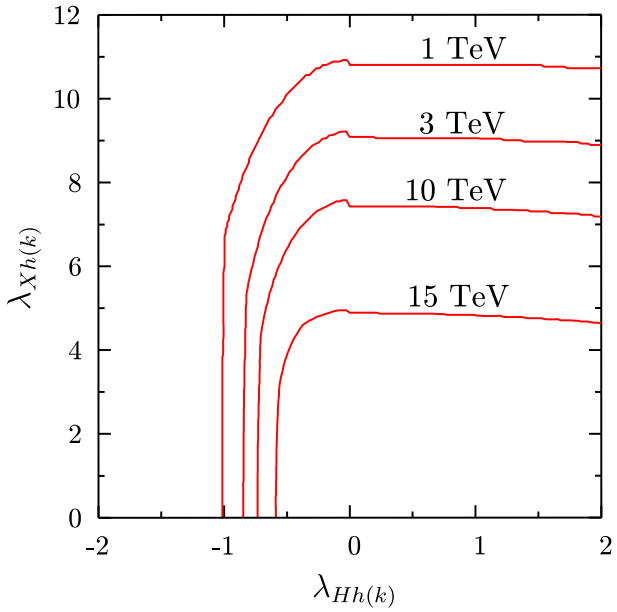

Figure 1. The perturbativity bounds, $\lambda_i(Q) < 4\pi$ are shown. The each curve denotes $Q = 1$, 3, 10 and 15 TeV from top to bottom. We take $\lambda_{Hh} = \lambda_{Hk}$, $\lambda_{Xh} = \lambda_{Xk}$, $\lambda_{hk} = \lambda_{HX} = 0$ and $\lambda_X = \lambda_H (\simeq 0.13)$. For the negative λ_{Hk}, we set $\lambda_h = \lambda_{Hh}^2/(2\lambda_H)$ and $\lambda_k = \lambda_{Hk}^2/(2\lambda_H)$ while $\lambda_h = \lambda_k = \lambda_H$ for positive λ_{Hk}.

3 Dark matter phenomenology and $H \to \gamma\gamma$

3.1 $XX \to \gamma\gamma$ and Fermi/LAT 130 GeV γ-ray excess

The annihilation cross section for $XX \to \gamma\gamma$ is given by

$$\langle \sigma v \rangle_{\gamma\gamma} = \frac{\sum |\mathcal{M}|^2}{64\pi m_X^2}, \tag{3.1}$$

where the amplitude-squared summed over the photon polarization is

$$\begin{aligned}\sum |\mathcal{M}|^2 = \frac{\alpha^2}{2\pi^2}\Bigg| & - \lambda_{Xh}\tau_{h^+}A_0(\tau_{h^+}) - 4\lambda_{Xk}\tau_{k^{++}}A_0(\tau_{k^{++}}) \\ & + \frac{\lambda_{HX}v^2}{4m_X^2 - m_H^2}\left[\frac{g^2}{2}\tau_W\Big(Q_t^2 N_C A_{1/2}(\tau_t) + A_1(\tau_W)\Big)\right. \\ & \left. - \lambda_{Hh}\tau_{h^+}A_0(\tau_{h^+}) - 4\lambda_{Hk}\tau_{k^{++}}A_0(\tau_{k^{++}})\right]\Bigg|^2,\end{aligned} \tag{3.2}$$

with $\tau_i = m_X^2/m_i^2 (i = h^+, k^{++}, t, W)$. The loop functions are

$$\begin{aligned} A_0(\tau) &= -\Big[\tau - f(\tau)\Big]\tau^{-2}, \\ A_{1/2}(\tau) &= 2\Big[\tau + (\tau - 1)f(\tau)\Big]\tau^{-2}, \\ A_1(\tau) &= -\Big[2\tau^2 + 3\tau + 3(2\tau - 1)f(\tau)\Big]\tau^{-2}, \end{aligned} \tag{3.3}$$

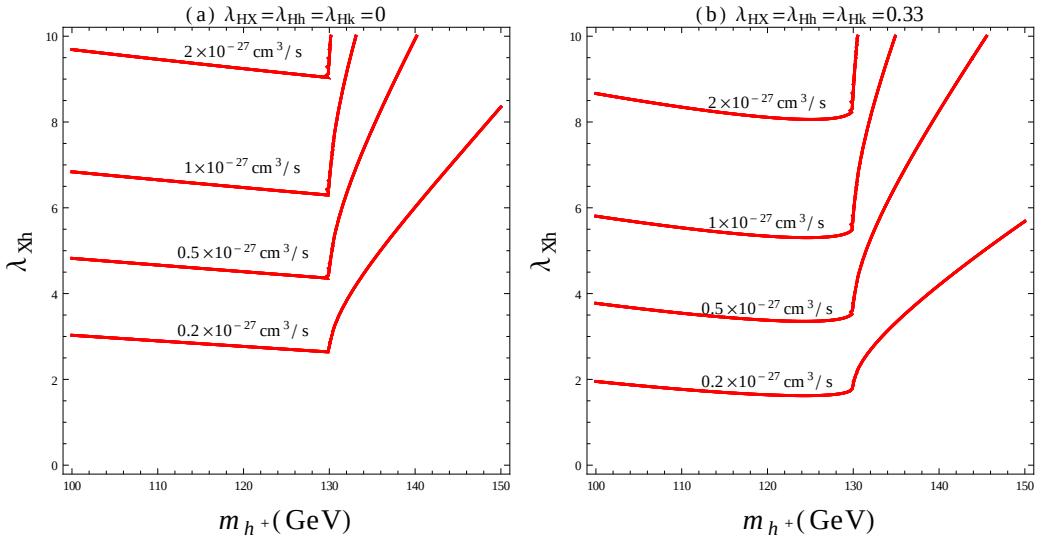

Figure 2. Contour plot of $\langle\sigma v\rangle_{\gamma\gamma} = (2, 1, 0.5, 0.2)\times10^{-27}\text{cm}^3/\text{s}$ (from above) in (m_{h^+}, λ_{Xh}) plane. We set $m_X = 130$ GeV, $m_H = 125$ GeV, $m_k = 500$ GeV and $\lambda_{Xk} = 5, \lambda_{HX} = \lambda_{Hh} = \lambda_{Hk} = 0(0.33)$ in the left (right) panel.

where

$$f(\tau) = \begin{cases} \arcsin^2\sqrt{\tau}, & (\tau \le 1) \\ -\frac{1}{4}\left[\log\frac{1+\sqrt{1-\tau^{-1}}}{1-\sqrt{1-\tau^{-1}}} - i\pi\right]^2, & (\tau > 1). \end{cases} \tag{3.4}$$

Although the contribution of the doubly-charged Higgs k^{++} to $\langle\sigma v\rangle_{\gamma\gamma}$ is $2^4 = 16$ times larger than that of the singly-charged Higgs h^+ when their masses are similar to each other, this option is ruled out by the recent LHC searches for the doubly-charged Higgs boson [13]. Depending on the decay channels, the 95% CL lower limit on the mass of the doubly-charged Higgs boson is in the range, 204–459 GeV. To be conservative, we set $m_{k^{++}} = 500$ GeV. In Figure 2, we show a contour plot for the annihilation cross section into two photons: $\langle\sigma v\rangle_{\gamma\gamma} \approx (2, 1, 0.5, 0.2)\times10^{-27}\text{cm}^3/\text{s}$ (from above) in the (m_{h^+}, λ_{Xh}) plane. We set $m_X = 130$ GeV, $m_H = 125$ GeV, $m_{k^{++}} = 500$ GeV and $\lambda_{Xk} = 5, \lambda_{HX} = \lambda_{Hh} = \lambda_{Hk} = 0$ (0.33) in the left (right) panel. We can see that even with $\lambda_{HX} = 0.33$, the process $XX \to H \to \gamma\gamma$ can be significant. However, this value of λ_{HX} produces too large cross section to explain the current CDM relic density, and and we would need another DM components. We can see that the Fermi result can be explained when m_{h^+} lies in the range 100–135 (150) GeV for $\lambda_{Xk} \sim 5$ with the cross section $\langle\sigma v\rangle_{\gamma\gamma} \approx 1(0.2)\times10^{-27}\text{cm}^3/\text{s}$. In this case the cut-off scale can be as large as 15 TeV (See Fig. 1). This mass range is within the reach of the on-going LHC experiments. And the model can be tested soon.

3.2 Direct detection rate and thermal relic density

Contrary to J. Cline's model [6], the DM relic density in our model is not necessarily correlated with the $\langle\sigma v\rangle_{\gamma\gamma}$, since it is mainly determined by λ_{HX} for relatively heavy scalars ($\gtrsim 150$ GeV). In this case the main DM annihilation channels are $XX \to H \to$ SM particles,

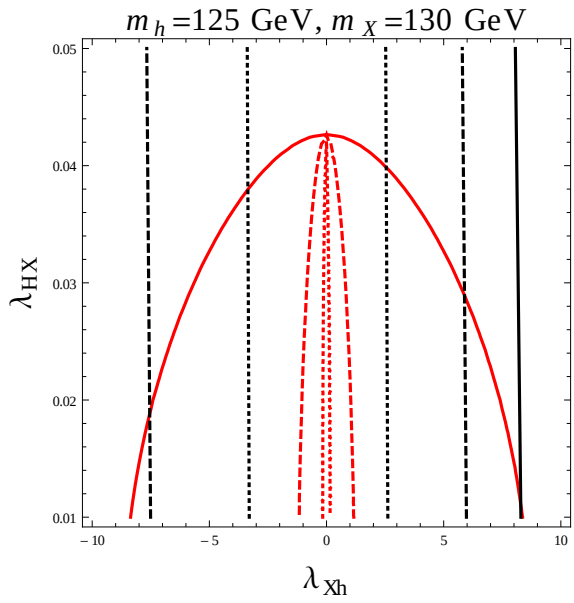

Figure 3. The contour plot of $\Omega_{\rm DM}h^2 = 0.1123$ (red lines) and $\langle\sigma v\rangle_{\gamma\gamma} = 0.2 \times 10^{-27}{\rm cm}^3/{\rm s}$ (black lines) in the (λ_{Xh},λ_{HX}) plane for the choices m_{h^+} 150, 140, 130 GeV (solid, dashed, dotted lines). For other parameters we set $m_X = 130$ GeV, $m_H = 125$ GeV, $m_k = 500$ GeV, $\lambda_{Xk} = 5$, $\lambda_{Hh} = \lambda_{Hk} = 0.5$.

where the SM particles are W^+W^-, ZZ, $b\bar{b}$, *etc.* As $m_{h^+(k^{++})}$ becomes comparable with m_X, the $XX \to h^+h^-(k^{++}k^{--})$ modes can open, even in cases $m_X < m_{h^+}(m_{k^{++}})$ thanks to the kinetic energy of X at freeze-out time. This can be seen in Figure 3, where we show the contour plot of $\Omega_{\rm DM}h^2 = 0.1123$ (red lines) in the (λ_{Xh},λ_{HX}) plane for the choices $m_{h^+} = 150$, 140, 130 GeV (shown in solid, dashed, dotted lines respectively). We fixed other parameters to be $m_X = 130$ GeV, $m_H = 125$ GeV, $m_k = 500$ GeV, $\lambda_{Xk} = 5$, $\lambda_{Hh} = \lambda_{Hk} = 0.5$. For $m_{h^+} = 130$ GeV, the annihilation mode $XX \to h^+h^-$ dominates even for very small coupling λ_{Xh} (the red dotted line). The black vertical lines are the constant contour lines of $\langle\sigma v\rangle_{\gamma\gamma} = 0.2 \times 10^{-27}{\rm cm}^3/{\rm s}$. Again the solid (dashed, dotted) line is for $m_{h^+} = 150$ (140, 130) GeV.

For $m_{h^+} = 150$ GeV, black line meets the red line, which means that if $\langle\sigma v\rangle_{\gamma\gamma}$ turns out to be about $0.2 \times 10^{-27}{\rm cm}^3/{\rm s}$ in future experiments, our model can both explain the Fermi/LAT result and saturate the relic density. Otherwise, the $\langle\sigma v\rangle_{\gamma\gamma}$ remain as large as the current value, the relic density is too small to explain the observed value and we need other DM components. For $m_{h^+} = 130, 140$ GeV, even $\langle\sigma v\rangle_{\gamma\gamma} = 0.2 \times 10^{-27}{\rm cm}^3/{\rm s}$ is too large to saturate the relic density.

Figure 4 shows the cross section of dark matter scattering off proton, σ_p, as a function of λ_{HX} (red solid line) and $\sigma_p = 1.5 \times 10^{-8}$ pb line (black dashed line) above which is excluded by XENON100 [14] at 90% C.L. This cross section is determined basically only by λ_{HX} at tree level by the SM Higgs exchange, when we fix $m_X = 130$ GeV. We can see that $\lambda_{HX} \lesssim 0.1$ to satisfy the XENON100 upper bound. We see that the cross section is close to the current bound and can be probed by near-future experiments when $\lambda_{HX} \gtrsim 0.02$.

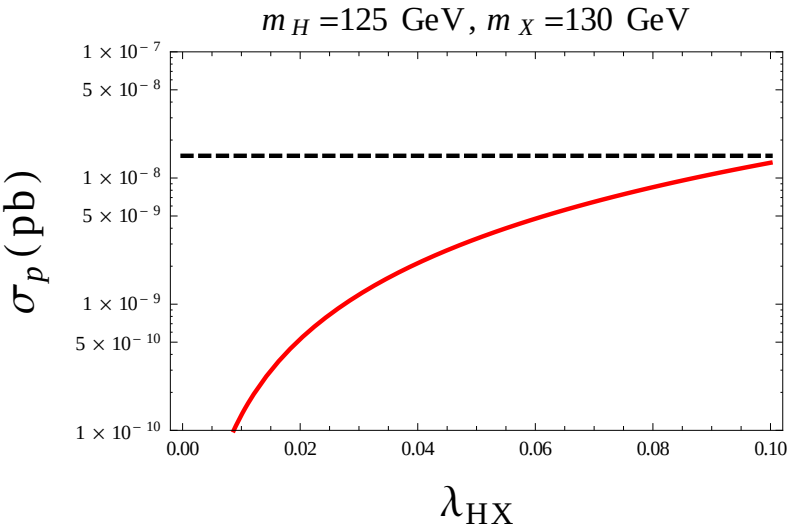

Figure 4. The spin-independent cross section of dark matter scattering off proton, σ_p, as a function of λ_{HX} (red solid line) and $\sigma_p = 1 \times 10^{-8}$ pb line above which is excluded by XENON100 (black dashed line). We take $m_H = 125$ GeV and $m_X = 130$ GeV.

If the new scalars are light and dominate the DM annihilation cross section for the relic density, we have $\lambda_{HX} \lesssim 0.02$ and the σ_p is one order of magnitude less than the current bound.

3.3 $H \to \gamma\gamma$

In our model the decay width of $H \to \gamma\gamma$ is modified, whereas other Higgs decay widths are intact:

$$\Gamma(H \to \gamma\gamma) = \frac{G_F \alpha^2 m_H^3}{128\sqrt{2}\pi^3} \left| \sum_{f=t,b} Q_f^2 N_c A_{1/2}(\tau_f) + A_1(\tau_W) + \frac{\lambda_{Hh} m_W v}{g m_{h^+}^2} A_0(\tau_{h^+}) + \frac{4\lambda_{Hk} m_W v}{g m_{k^{++}}^2} A_0(\tau_{k^{++}}) \right|^2 , \tag{3.5}$$

where $\tau_i = m_H^2/4m_i^2$ $(i = f, W, h^+, k^{++})$.

In Figure 5, we show contour plots for constant $\Gamma(H \to \gamma\gamma)/\Gamma(H \to \gamma\gamma)^{\rm SM}$ (black solid lines) and $\Gamma(H \to Z\gamma)/\Gamma(H \to Z\gamma)^{\rm SM}$ (black dashed lines) in the $(\lambda_{Hh}, \lambda_{Hk})$ plane. For this plot we set $m_{h^+} = 130$ (150) GeV for the left (right) panel and fixed $m_{k^{++}} = 500$ GeV. The shaded regions are disfavored by (2.5) (blue) and by (2.7) (yellow). Given that $\lambda_{HX} \lesssim 0.1$ by the direct detection experiments, the ratio depends basically only on the coupling constants λ_{Hh} and λ_{Hk} as well as the masses m_{h^+} and $m_{k^{++}}$. In our model the ratio is not necessarily correlated with the $\langle\sigma v\rangle_{\gamma\gamma}$ which are controlled by λ_{Xh} and λ_{Xk}. We can conclude that

$$\begin{aligned} 0.54 \lesssim\ & \Gamma(H \to \gamma\gamma)/\Gamma(H \to \gamma\gamma)^{\rm SM} \lesssim 1.45\ (1.35) \\ 0.91 \lesssim\ & \Gamma(H \to Z\gamma)/\Gamma(H \to Z\gamma)^{\rm SM} \lesssim 1.11\ (1.08) \end{aligned}$$

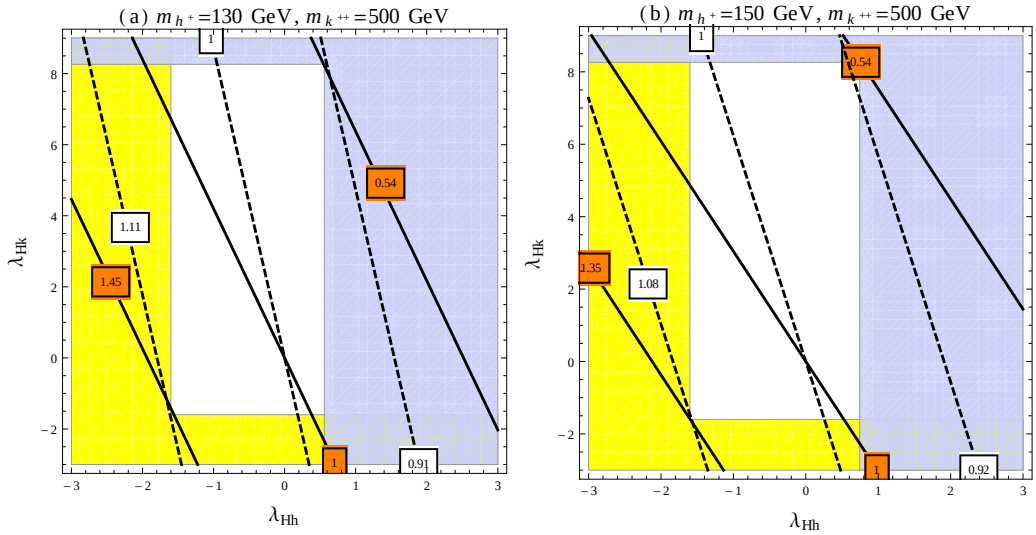

Figure 5. A contour plot for constant $\Gamma(H \to \gamma\gamma)/\Gamma(H \to \gamma\gamma)^{\rm SM}$ (black solid lines) and $\Gamma(H \to Z\gamma)/\Gamma(H \to Z\gamma)^{\rm SM}$ (black dashed lines) in the $(\lambda_{Hh}, \lambda_{Hk})$ plane. The shaded regions are disfavored by (2.5) (blue) and by (2.7) (yellow). We set $m_{h^+} = 130$ (150) GeV for the left (right) panel and fixed $m_{k^{++}} = 500$ GeV.

for the left (right) panel. That is, the $H \to \gamma\gamma$ channel can be enhanced (reduced) significantly, whereas the $H \to Z\gamma$ channel can change only upto $\sim 10\%$.

3.4 Implications for neutrino physics

So far, we did not consider the constraints from neutrino sector and charged lepton flavor violation. In fact, these constraints are rather severe, if we assume that the observed neutrino masses and mixings are entirely from the Zee-Babu mechanism. One cannot afford light $h^\pm$ or $k^{\pm\pm}$, because of the constraints from charged LFV: $m_{h^+} \gtrsim 240$ GeV from $B(\mu \to e\gamma) < 2.4 \times 10^{-12}$ [15] and $m_{k^{++}} \gtrsim 770$ GeV from the upper bound on $\tau \to 3\mu$ decay [10].

If we insist that the Fermi/LAT excess is due to the light $h^\pm$ loop, then we get $\mu_{hk} \gtrsim 14$ TeV, which is inconsistent with the constraint $\mu_{hk} \lesssim 450$ GeV from the vacuum stability bound [9]. And there should be additional contributions to neutrino masses, such as from dim-5 Weinberg operators. If these dim-5 operators are induced through Type-I seesaw mechanism, the new physics would not affect our conclusion. On the other hand, if the dim-5 operators are induced by TeV scale seesaw, then the new physics from TeV scale seesaw might affect our conclusions.

Although it is not very satisfactory that the original Zee-Babu model with scalar dark matter cannot explain both the Fermi/LAT 130 GeV γ ray excess and neutrino physics simultaneously, it would be more natural to consider the Zee-Babu model as a low energy effective theory. Then it would be natural there could be new contributions to the neutrino masses and mixings from dim-5 operators. The only relevant question would be whether those new physics would affect the Fermi/LAT γ-ray or not. If the new physics is Type-I seesaw, there would be no new charged particles so that our conclusion would remain valid.

4 Conclusions

We have minimally extended the 'Zee-Babu model' [7–9] incorporating a scalar dark matter X with Z_2 symmetry under $X \to -X$. If the scalar dark matter X has a mass around 130 GeV, it can explain a recent claim that Fermi gamma-ray space telescope has seen an excess in gamma line at 130 GeV. If the excess is interpreted as the annihilation of a dark matter pair into two photons, the estimated cross section $\langle\sigma v\rangle_{\gamma\gamma} \approx 1 \times 10^{-27}\text{cm}^3/\text{s}$ can be explained by the contribution of the singly- and/or doubly-charged Higgs present in the model.

We have shown that the present constraint on the couplings λ_{Xk} and λ_{Xh} which mix the dark matter and charged Higgs is not so strong and they can enhance the annihilation cross section of $XX \to \gamma\gamma$ large enough to accommodate the recent hint. On the other hand the couplings which involve the SM Higgs H are strongly constrained by the theoretical considerations in the Higgs potential and the observations of dark matter relic density and dark matter direct detections. The strongest upper bound on the λ_{HX} coupling is about 0.1 which comes from the dark matter direct detection experiments. For the $\lambda_{Hh}, \lambda_{Hk}$ which mix the SM Higgs and the new charged Higgs, the theoretical bound becomes more important. If we require the absolute stability of the dark matter by the Z_2 symmetry $X \to -X$ and the absence of charge breaking, we get the upper bound of $\lambda_{Hh}, \lambda_{Hk}$ to be about 0.7 for the charged Higgs mass around 150 GeV. To evade the unbounded-from-below Higgs potential we need to have $\lambda_{Hh}, \lambda_{Hk} \gtrsim -1.6$.

With these constraints the $B(H \to \gamma(Z)\gamma)$ can be enhanced up to 1.5 (1.1) or suppressed down to 0.5 (0.9) with respect to that in the SM. The direct detection cross section of X is suppressed by more than an order of magnitude to the current XENON100 bound if we want to saturate the relic density.

However the neutrino sector cannot be described by the Zee-Babu model only, and there should be additional contributions to the neutrino masses and mixings such as dimension-5 Weinberg operator from type-I seesaw mechanism. As long as the new mechanism does not involve new charged particles around EW scale, our predictions for 130 GeV γ-ray excess and the enhanced $B(H \to \gamma\gamma)$ would be still valid.

Acknowledgments

This work is partly supported by NRF Research Grant 2012R1A2A1A01006053 (PK, SB).

A One-loop β functions of the quartic couplings

Here, we give the renormalization group equation and the one-loop β functions of the quartic couplings:

$$\frac{d\lambda_i}{d\ln Q} = \beta_{\lambda_i}, \tag{A.1}$$

with

$$\beta_{\lambda_H} = \frac{1}{16\pi^2}\Bigg[24\lambda_H^2 + \lambda_{Hh}^2 + \lambda_{Hk}^2 + \frac{\lambda_{HX}^2}{2} - 6y_t^4 + \frac{3}{8}\Big\{2g_2^4 + (g_2^2+g_1^2)^2\Big\} - 4\lambda_H\left\{\frac{3}{4}(3g_2^2+g_1^2) - 3y_t^2\right\}\Bigg], \tag{A.2}$$

$$\beta_{\lambda_h} = \frac{1}{16\pi^2}\left[16\lambda_h^2 + 2\lambda_{Hh}^2 + \lambda_{hk}^2 + \frac{\lambda_{Xh}^2}{2} + 6g_1^4 - 12\lambda_h g_1^2\right], \tag{A.3}$$

$$\beta_{\lambda_k} = \frac{1}{16\pi^2}\left[16\lambda_k^2 + 2\lambda_{Hk}^2 + \lambda_{hk}^2 + \frac{\lambda_{Xk}^2}{2} + 96g_1^4 - 48\lambda_k g_1^2\right], \tag{A.4}$$

$$\beta_{\lambda_X} = \frac{1}{16\pi^2}\Big[18\lambda_X^2 + 2\lambda_{HX}^2 + \lambda_{Xh}^2 + \lambda_{Xk}^2\Big], \tag{A.5}$$

$$\beta_{\lambda_{Hh}} = \frac{1}{16\pi^2}\Bigg[12\lambda_H\lambda_{Hh} + 8\lambda_h\lambda_{Hh} + 2\lambda_{hk}\lambda_{Hk} + \lambda_{HX}\lambda_{Xh} + 3g_1^4 - \lambda_{Hh}\left\{\frac{3}{2}(3g_2^2+g_1^2) - 6y_t^2 + 6g_1^2\right\}\Bigg], \tag{A.6}$$

$$\beta_{\lambda_{Hk}} = \frac{1}{16\pi^2}\Bigg[12\lambda_H\lambda_{Hk} + 8\lambda_k\lambda_{Hk} + 2\lambda_{hk}\lambda_{Hh} + \lambda_{HX}\lambda_{Xk} + 12g_1^4 - \lambda_{Hk}\left\{\frac{3}{2}(3g_2^2+g_1^2) - 6y_t^2 + 24g_1^2\right\}\Bigg], \tag{A.7}$$

$$\beta_{\lambda_{hk}} = \frac{1}{16\pi^2}\Big[4\lambda_{Hh}\lambda_{Hk} + 8\lambda_{hk}(\lambda_h+\lambda_k) + \lambda_{Xh}\lambda_{Xk} + 48g_1^4 - 30\lambda_{hk}g_1^2\Big], \tag{A.8}$$

$$\beta_{\lambda_{HX}} = \frac{1}{16\pi^2}\left[12\lambda_H\lambda_{HX} + 2\lambda_{Hh}\lambda_{Xh} + 2\lambda_{Hk}\lambda_{Xk} + 6\lambda_X\lambda_{HX} - \lambda_{HX}\left\{\frac{3}{2}(3g_2^2+g_1^2) - 6y_t^2\right\}\right], \tag{A.9}$$

$$\beta_{\lambda_{Xh}} = \frac{1}{16\pi^2}\Big[4\lambda_{Hh}\lambda_{HX} + 8\lambda_h\lambda_{Xh} + 2\lambda_{hk}\lambda_{Xk} + 6\lambda_X\lambda_{Xh} - 6\lambda_{Xh}g_1^2\Big], \tag{A.10}$$

$$\beta_{\lambda_{Xk}} = \frac{1}{16\pi^2}\Big[4\lambda_{Hk}\lambda_{HX} + 8\lambda_k\lambda_{Xk} + 2\lambda_{hk}\lambda_{Xh} + 6\lambda_X\lambda_{Xk} - 24\lambda_{Xk}g_1^2\Big]. \tag{A.11}$$

References

[1] N. Jarosik, C. L. Bennett, J. Dunkley, B. Gold, M. R. Greason, M. Halpern, R. S. Hill, G. Hinshaw *Eu AB.*, Astrophys. J. Suppl. **192**, 14 (2011). [arXiv:1001.4744 [astro-ph.CO]].

[2] Y. .B. Zeldovich, A. A. Klypin, M. Y. .Khlopov and V. M. Chechetkin, Sov. J. Nucl. Phys. **31**, 664 (1980) [Yad. Fiz. **31**, 1286 (1980)].

[3] T. Bringmann, X. Huang, A. Ibarra, S. Vogl and C. Weniger, arXiv:1203.1312 [hep-ph].

[4] C. Weniger, arXiv:1204.2797 [hep-ph].

[5] E. Tempel, A. Hektor and M. Raidal, arXiv:1205.1045 [hep-ph]; E. Dudas, Y. Mambrini, S. Pokorski and A. Romagnoni, arXiv:1205.1520 [hep-ph]; J. M. Cline, arXiv:1205.2688 [hep-ph]; K. -Y. Choi and O. Seto, Phys. Rev. D **86**, 043515 (2012) [arXiv:1205.3276 [hep-ph]]; B. Kyae and J. -C. Park, arXiv:1205.4151 [hep-ph]; H. M. Lee, M. Park and W. -I. Park, arXiv:1205.4675 [hep-ph]; B. S. Acharya, G. Kane, P. Kumar, R. Lu and B. Zheng, arXiv:1205.5789 [hep-ph]; M. R. Buckley and D. Hooper, Phys. Rev. D **86**,

043524 (2012) [arXiv:1205.6811 [hep-ph]]; X. Chu, T. Hambye, T. Scarna and M. H. G. Tytgat, arXiv:1206.2279 [hep-ph]; D. Das, U. Ellwanger and P. Mitropoulos, JCAP **1208**, 003 (2012) [arXiv:1206.2639 [hep-ph]]. D. Das, U. Ellwanger and P. Mitropoulos, JCAP **1208**, 003 (2012) [arXiv:1206.2639 [hep-ph]]; Z. Kang, T. Li, J. Li and Y. Liu, arXiv:1206.2863 [hep-ph]; N. Weiner and I. Yavin, arXiv:1206.2910 [hep-ph]; L. Feng, Q. Yuan and Y. -Z. Fan, arXiv:1206.4758 [astro-ph.HE]; W. Buchmuller and M. Garny, JCAP **1208**, 035 (2012) [arXiv:1206.7056 [hep-ph]]; J. H. Heo and C. S. Kim, arXiv:1207.1341 [astro-ph.HE]; E. Hardy, J. March-Russell and J. Unwin, arXiv:1207.1435 [hep-ph]; M. T. Frandsen, U. Haisch, F. Kahlhoefer, P. Mertsch and K. Schmidt-Hoberg, arXiv:1207.3971 [hep-ph]; J. -C. Park and S. C. Park, arXiv:1207.4981 [hep-ph]; S. Tulin, H. -B. Yu and K. M. Zurek, arXiv:1208.0009 [hep-ph]; T. Li, J. A. Maxin, D. V. Nanopoulos and J. W. Walker, arXiv:1208.1999 [hep-ph]; J. M. Cline, A. R. Frey and G. D. Moore, arXiv:1208.2685 [hep-ph]; Y. Bai and J. Shelton, arXiv:1208.4100 [hep-ph]; R. Laha, K. C. Y. Ng, B. Dasgupta and S. Horiuchi, arXiv:1208.5488 [astro-ph.CO]; L. Bergstrom, arXiv:1208.6082 [hep-ph]; L. Wang and X. -F. Han, arXiv:1209.0376 [hep-ph].

[6] J. M. Cline, in Ref. [5]

[7] A. Zee, Nucl. Phys. B **264**, 99 (1986).

[8] K. S. Babu, Phys. Lett. B **203**, 132 (1988).

[9] K. S. Babu and C. Macesanu, Phys. Rev. D **67**, 073010 (2003) [hep-ph/0212058].

[10] D. Aristizabal Sierra and M. Hirsch, JHEP **0612**, 052 (2006) [hep-ph/0609307].

[11] M. Lindner, D. Schmidt and T. Schwetz, Phys. Lett. B **705**, 324 (2011) [arXiv:1105.4626 [hep-ph]].

[12] S. Chatrchyan *et al.* [CMS Collaboration], Phys. Lett. B **710**, 26 (2012) [arXiv:1202.1488 [hep-ex]].

[13] S. Chatrchyan *et al.* [CMS Collaboration], arXiv:1207.2666 [hep-ex].

[14] E. Aprile *et al.* [XENON100 Collaboration], Phys. Rev. Lett. **107**, 131302 (2011) [arXiv:1104.2549 [astro-ph.CO]].

[15] J. Beringer *et al.* [Particle Data Group Collaboration], Phys. Rev. D **86**, 010001 (2012).